Available online at www.sciencedirect.com
ScienceDirect
Archives of Biochemistry and Biophysics XX-XX
ABB
www.elsevier.com/locate/yabbi

Cellular death linked to irreversible stress in the sarcoplasmic reticulum: The effect of inhibiting Ca^{2+}–ATPase or protein glycosylation in the myocardiac cell model H9c2

Fernando Soler [1], Antonio Lax [1], Francisco Fernández-Belda *

Departamento de Bioquímica y Biología Molecular A, Universidad de Murcia, Campus de Espinardo, 30071 Murcia, Spain

Received 3 May 2007, and in revised form 25 June 2007

Abstract

Experimental sarcoplasmic reticulum damage induced by 3 μM thapsigargin or 1 μg/ml tunicamycin provoked viability loss of the cell population in approximately 72 h. Release of cytochrome *c* from mitochondria was an early event and Bax translocation to the mitochondria preceded or was simultaneous with cytochrome *c* release. The release of cytochrome *c* was not related with mitochondria depolarization or caspase activation. Irreversible stress in the sarcoplasmic reticulum, detected by the early activation of caspase 12, was functionally linked to the mitochondrial apoptotic pathway. Caspase 3 processing was blocked by cells preincubation with a selective inhibitor of either caspase 9 or caspase 8 whereas caspase 8 activation was inhibited by a selective caspase 9 inhibitor. This was consistent with the involvement of caspase 8 in a positive feedback loop leading to amplify the caspase cascade. Caspase inhibition did not protect against cell death indicating the existence of alternative caspase-independent mechanisms.

Keywords: Ca^{2+}–ATPase inhibition; Thapsigargin; Tunicamycin; Sarcoplasmic reticulum; Cell death; Cardiac cell line

Apoptosis is a highly regulated process used by multicellular organisms for the physiological removal of unwanted cells. It plays a critical role during prenatal development but also operates in the postnatal life being responsible for cell turnover and tissue homeostasis [1]. Eukaryotic cells are endowed with a number of mechanisms that can detect and respond to specific local damages. When the protective responses that can be orchestrated by the cell are insufficient to cope with the alterations the apoptotic process ensues. Plasma membrane receptors [2] and mitochondrion [3] were first recognized to detect specific stress signals that eventually resulted in the demise of the cell. Organelles other than the mitochondrion such as nucleus, endoplasmic reticulum (ER)[2] or the muscle cell counterpart sarcoplasmic reticulum (SR) and the Golgi apparatus can detect and initiate cell death responses [4]. It seems that cells are maintained alive by a delicate balance between opposing signals designed to maintain life or induce death [5].

* Corresponding author. Fax: +34 968 364 147.
E-mail address: fbelda@um.es (F. Fernández-Belda).
[1] These authors contributed equally to this work.
[2] *Abbreviations used*: ER, endoplasmic reticulum; SR, sarcoplasmic reticulum; TG, thapsigargin; TM, tunicamycin; MTT, 3-(4,5-dimethylthiazol-2-yl)-2,5-diphenyltetrazolium bromide; JNK, c-jun amino-terminal kinase; casp, caspase; cyt *c*, cytochrome *c*; COX IV, cytochrome oxidase, complex IV; DMEM, Dulbecco's modified Eagle's medium; PBS, phosphate-buffered saline; PBST, phosphate-buffered saline supplemented with Tween 20; $\Delta\Psi_m$, inner mitochondrial membrane potential; CsA, cyclosporin A; CCCP, carbonyl cyanide *m*-chlorophenylhydrazone; PTP, permeability transition pore; JC-1, 5,5′,6,6′-tetrachloro-1,1′,3,3′-tetraethylbenzimidazolylcarbocyanine iodide; HEPES, 4-(2-hydroxyethyl)piperazine-1-ethanesulfonic acid; Bax, Bcl-2-associated X protein; z-VAD-fmk, *N*-benzyloxycarbonyl-Val-Ala-Asp(OCH_3)-fluoromethylketone; z-LEHD-fmk, *N*-benzyloxycarbonyl-Leu-Glu(OCH_3)-His-Asp(OCH_3)-fluoromethylketone; z-IETD-fmk, *N*-benzyloxycarbonyl-Ile-Glu(OCH_3)-Thr-Asp(OCH_3)-fluoromethylketone.

0003-9861/$ - see front matter

Cardiac myocytes are terminally differentiated cells and therefore the induction of the apoptotic process is expected to have a significant impact on cardiac performance. Apoptosis of myocardiac cells has been implicated in the pathogenesis of several heart dysfunctions related with infarction [6], ischemia–reperfusion [7], pressure overload [8] and chronic heart failure [9], although the precise contribution to disease states remains to be established.

The SR of myocardiac cells is the source where cytosolic Ca^{2+} signals involved in heart contraction are originated and the place where synthesis, folding and modification of secretory and membrane proteins occur. Diminution of the intracellular ATP content as that occurring during an ischemic episode decreases the SR Ca^{2+} reserve thereby limiting the function of some SR chaperone proteins [10]. Protein synthesis, folding mediated by SR chaperone and modifications including glycosylation are also affected [10]. Consequently, disruption of the SR function is expected to initiate the unfolded protein response as it has been described for the ER [11]. When the protective response launched by the cell cannot restore the physiological conditions a SR stress-dependent suicide program is unleashed. The current knowledge of this complex and step-wise process is sketchy and most of the available data come from cell types other than myocardiac.

To identify potential therapeutic targets, it is imperative to have a full understanding of the apoptotic processes that are operative in myocardiac cells. Experimentally induced SR damage was achieved by addition of thapsigargin (TG), a naturally occurring sesquiterpene lactone displaying high affinity inhibition on SR/ER Ca^{2+}–ATPase [12], or tunicamycin (TM), a pharmacological inhibitor of the N-linked glycosylation of proteins that takes place in the SR/ER. Irreversible disruption of the SR Ca^{2+} pool by direct action of TG and not by decreasing the intracellular ATP content avoided undesirable effects on many other key events that are energy-dependent.

The effect of TG and TM as inducers of SR stress-dependent apoptosis has been studied in a culture of H9c2 cells. This perennial cell line displays morphological features of immature embryonic cardiomyocytes but retains many functional elements of adult myocardiac cells including the evolutionarily conserved signaling cascades. In fact, H9c2 cells have been used to evaluate biochemical responses induced by pathological conditions of the heart such as the role of the c-jun amino-terminal kinase (JNK) pathway in the apoptotic death induced by oxidative stress [13], the mitogen-activated protein kinase pathway during post-ischemic reperfusion [14] or the hypertrophic growth induced by increased work load and mediated by upregulation of the transforming growth factor-β [15].

Materials and methods

Materials

Rat heart-derived H9c2 cells [16] were obtained from the European Collection of Cell Cultures (www.ecacc.org.uk). The nitrocellulose transfer membrane Protran® BA 83 was supplied by Schleicher & Schuell BioScience. Image-iT™ FX Signal Enhancer was a product of Molecular Probes™. Chemichrome Western Control (C 2242) and the Chemiluminescent Peroxidase Substrate (CPS-1-120) were from Sigma. Qentix™ Western Blot Signal Enhancer was from Pierce and Curix RP2 plus film was from Agfa.

Reagents and media

Culture reagents including Dulbecco's modified Eagle's medium (DMEM) with low glucose and L-glutamine, fetal bovine serum and penicillin–streptomycin–L-glutamine mixture were from Gibco. The cell dissociation solution containing 0.25% trypsin was also from Gibco. TG, TM from *Streptomyces* sp., cyclosporin A (CsA), and the protease inhibitor cocktail (P 8340) were obtained from Sigma. 5,5′,6,6′-tetrachloro-1,1′,3,3′-tetraethylbenzimidazolylcarbocyanine iodide (JC-1) and MitoTracker® Red CM-H_2XRos were from Molecular Probes™. *N*-benzyloxycarbonyl-Val-Ala-Asp(OCH_3)-fluoromethylketone (z-VAD-fmk) and *N*-benzyloxycarbonyl-Ile-Glu(OCH_3)-Thr-Asp(OCH_3)-fluoromethylketone (z-IETD-fmk) were purchased from Bachem whereas *N*-benzyloxycarbonyl-Leu-Glu(OCH_3)-His-Asp(OCH_3)-fluoromethylketone (z-LEHD-fmk) was from BD Pharmingen. All other chemicals were of analytical grade and also provided by Sigma.

The permeabilization medium for digitonin treatment was 250 mM sacarose, 75 mM KCl, 1 mM NaH_2PO_4 and 8 mM Na_2HPO_4. The solubilization medium after the digitonin treatment was 150 mM Tris–HCl, 1 mM EGTA, 1% Triton X-100, 1% sodium deoxycholate and 0.1% SDS at pH 8.0. The sample buffer for electrophoresis was 62.5 mM Tris–HCl, 2% SDS, 5% β-mercaptoethanol, 7.5% glycerol and 0.0003% bromophenol blue at pH 6.8. Phosphate-buffered saline (PBS) was 137 mM NaCl, 2.7 mM KCl, 10.14 mM Na_2HPO_4 and 1.76 mM KH_2PO_4 adjusted to pH 7.4 with HCl. Phosphate-buffered saline supplemented with Tween 20 (PBST) was PBS containing 0.05% Tween 20. The blocking solution for blotted proteins was PBST supplemented with 5% skim dried milk. The stripping buffer for antibody reprobing was 62.5 mM Tris–HCl, 2% SDS and 100 mM β-mercaptoethanol at pH 6.8. The modified Tyrode's solution was 10 mM 4-(2-hydroxyethyl)piperazine-1-ethanesulfonic acid (HEPES)–NaOH, 121 mM NaCl, 4.7 mM KCl, 1 mM $CaCl_2$, 1.2 mM $MgSO_4$, 5 mM $NaHCO_3$, 1.2 mM KH_2PO_4, 10 mM glucose and 0.25% bovine serum albumin at pH 7.4.

Antibodies

Mouse anti-cytochrome *c* (cyt *c*) monoclonal antibody (clone 7H8.2C12) was purchased from BD Pharmingen. Mouse monoclonal antibody against cytochrome oxidase, complex IV (COX IV) and goat anti-mouse IgG linked to Alexa Fluor® 488 were from Molecular Probes™. Rabbit anti-caspase 12 (casp 12) polyclonal antibody (Ab-2) was purchased from Calbiochem and rabbit anti-casp 3 polyclonal antibody (H-277) was from Santa Cruz Biotechnology. Rabbit anti-casp 8 polyclonal antibody (AAP-118) was a product of Stressgen Bioreagents. Mouse anti-Bcl-2-associated X protein (Bax) monoclonal antibody (clone 6A7), mouse monoclonal anti-γ-tubulin (clone GTU-88) and the peroxidase-conjugated secondary antibodies rabbit anti-mouse IgG and goat anti-rabbit IgG were from Sigma.

H9c2 culture

Cells in complete culture medium consisting of DMEM, 10% heat-inactivated fetal bovine serum, 2 mM L-glutamine, 100 U/ml penicillin and 100 μg/ml streptomycin were maintained at 37 °C in growth exponential phase [17]. The monolayer culture was split at a 1:6 ratio or harvested to perform experiments when confluence was 70–80%. For induction of SR-mediated apoptosis, plated cells in DMEM were exposed to 3 μM TG or 1 μg/ml TM and maintained in the CO_2 incubator for defined periods of time.

MTT assay

Cells at $\sim 15 \times 10^3$/well were seeded in quadruplicate in 24-well plates and grown at 37 °C for 4 days in complete culture medium. Subconfluent

cultures in DMEM were subjected to the apoptotic treatment as described above. When indicated, cells were previously incubated with 20 μM z-VAD-fmk for 1 h. Culture medium from treated or untreated cells was aspirated and cells were washed twice with pre-warmed PBS. The redox potential of live cells was evaluated after incubation with 300 μl/well 1 mg/ml 3-(4,5-dimethylthiazol-2-yl)-2,5-diphenyltetrazolium bromide (MTT) for 30 min in the CO_2 incubator. The formazan precipitate was dissolved by adding 250 μl/well dimethyl sulfoxide and shaking the plate for 5 min at room temperature. Then, 25 μl of 2 M Tris at pH 10.5 was added to each well. Absorbance of the samples was read at 570 nm and the background value at 690 nm was subtracted. The index of cell survival at each time point in the absence or presence of apoptotic treatment corresponds to a percentage with respect to a time zero control.

JC-1 loading and flow-cytometry

Cells in one 150-mm plate at 70–80% confluence were subjected to the apoptotic protocol, as described above. Treated and untreated cells in DMEM were loaded at 37 °C for 10 min with 5 μg/ml JC-1. Then, cells were washed twice with pre-warmed PBS, trypsinized and resuspended at $\sim 3 \times 10^5$ cells/ml in modified Tyrode's solution at 25 °C. Measurements were immediately carried out in a Becton–Dickinson FACSort™ flow cytometer and samples were excited with the 488 nm line of a krypton/argon laser. The green and red fluorescence of JC-1 was detected through the FL-1 and FL-2 channels, respectively. Proper compensation was established to correct the fluorescence spillover [18]. The cell population under study was previously selected by electronic gating measuring forward vs. side light scatter. A total of 20,000 events were collected for the analysis of each sample. Data acquisition and analysis were performed with the CellQuest™ software from Becton–Dickinson.

Active Bax immunofluorescence

Cells ($\sim 2 \times 10^4$) were plated on each 35-mm glass bottom dish and grown at 37 °C in complete medium for 2 days. Adherent cells were washed twice with pre-warmed PBS and then incubated in DMEM with 3 μM TG for 0.5, 1 or 2 h. Treated and untreated cells were loaded at 37 °C for 45 min with 20 nM MitoTracker Red. This was followed by fixation with formaldehyde, permeabilization with Triton X-100 and treatment with the signal enhancer kit Image-iT™ FX according to the Molecular Probes' protocol. Cells were exposed overnight at 4 °C to mouse anti-Bax 6A7 (1:1000 dilution) and then to goat anti-mouse IgG conjugated to Alexa Fluor 488 (1:200 dilution) for 1 h at 37 °C. Labeled cells were viewed under a DM IRE II inverted fluorescence microscope from Leica Microsystems using HCX PL APO 63× oil immersion objective with numerical aperture 1.32. Alexa Fluor 488 and MitoTracker Red were excited with an argon-ion or green helium–neon laser beam, respectively. The corresponding ranges of emission wavelength were 510–550 nm and 590–650. Confocal images were collected with the Leica scanhead module TCS SP2. The pinhole aperture was set at 140 μm, equivalent to a *z* plane of 1.1 μm thickness.

Samples for protein detection

Subconfluent cultures in four 150-mm plates (~ 1.5 to 2×10^6 cells/plate) were left untreated or treated with the apoptotic inducer as described above. Then, cells were harvested at the appropriate time point, pooled and processed for the preparation of relevant cellular extracts. A bank of samples was systematically generated and maintained in the ultrafreezer at −80 °C for further use. Cyt *c* was studied in the S-10 and P-10 fractions, Bax in the P-10 fraction and the S-10 fraction was used for caspase detection.

Cellular extracts

The preparation of samples for protein detection was based on a previously described method for selective permeabilization of the plasma membrane [19]. Briefly, cells collected by centrifugation and washed twice in ice-cold PBS were resuspended at $\sim 4 \times 10^4$ cells/μl in ice-cold medium for permeabilization. The protease inhibitor cocktail at 4 μl/1×10^6 cells and digitonin to give 600 μg/ml were added. The incubation was maintained for 5 min in an ice bath. The digitonin treatment was empirically adjusted to get more than 95% of the cells stained with Trypan blue dye. Cells were centrifuged at 10,000*g* for 10 min and 4 °C and the supernatant was aliquoted, labeled as "S-10" and stored at −80 °C in the bank of samples. The pellet was resuspended in a volume of solubilization medium equal to the volume of medium for permeabilization previously used. The addition of protease inhibitor cocktail at 4 μl/1×10^6 cells and a brief sonication (4×5 s with 30 s intervals) at the ice-water temperature was followed by a new centrifugation at 10,000*g*. The resulting supernatant was aliquoted, labeled as "P-10" and frozen at −80 °C.

Protein determination

The protein content of the cellular extracts was measured by the bicinchoninic acid assay using bovine serum albumin as the standard protein [20].

Electrophoresis and Western blotting

The separation and detection of proteins was performed by standard procedures. Aliquots of soluble protein were initially boiled for 5–15 min in sample buffer. Thereafter, equal amounts of protein were resolved on 12% or 15% SDS–polyacrylamide gels [21] and electroblotted to nitrocellulose membrane using a semi-dry blotting apparatus from Bio-Rad. The protein transfer efficiency was checked by the chemichrome Western control mix. The membrane was treated with the signal enhancer kit from Pierce and then immersed at room temperature for 1 h in the blocking medium. The incubation with the primary antibody solution was prolonged overnight at 4 °C in a rocker. Antibodies against cyt *c*, casp 12 and γ-tubulin were used at 1:500. Anti-COX IV and anti-casp 8 antibodies were used at a dilution 1:1000 whereas anti-casp 3 was used at 1:200 and anti-Bax was 1:70. The membrane was washed three times for 5 min each with PBST and incubated again with blocking solution at room temperature for 30 min. Afterwards, the incubation with peroxidase-conjugated secondary antibody was maintained at room temperature for 1 h. Anti-mouse IgG was used at 1:20,000 and anti-rabbit IgG at 1:25,000. Following three new washes with PBST the immunoreactive bands were detected by the chemiluminescence method according to the Sigma's protocol. When indicated the blotting membrane was treated at 50 °C for 30 min with stripping buffer and then reexposed to anti-γ-tubulin, and in some cases also to anti-COX IV, followed by incubation with anti-mouse IgG linked to peroxidase.

Data presentation

Experimental data in the histograms are expressed as mean values of at least five independent assays and standard deviations are indicated by error bars. Differences were compared by the Student's *t*-test using the SigmaPlot 8.0 software. A value of $p < 0.05$ was considered to be significant. Western blots in the figures are representative of repeated experiments and have been reproduced using version 4.0 of the Adobe Photoshop software. None or minimal image treatment according to accepted guidelines [22] was applied. Flow-cytometry data presented as dots plot are representative of experiments performed at selected assay conditions. Time-dependent plots contain mean values from at least three experiments and the results are presented as percentage with respect to the selected cell population.

Results

The effect of TG or TM on cell damage is dependent on severity and duration of the apoptotic treatment. Thus,

incubation of H9c2 cells in DMEM with 3 μM TG led to time-dependent cell damage as evaluated by mitochondrial dysfunction with the MTT assay. Under these conditions, loss of viability in the cell population was completed in approximately 72 h (closed bars in Fig. 1a and Ref. [23]). It is also shown that the time course of cell damage in the presence of 1 μg/ml TM (closed bars in Fig. 1b) was similar to that induced by 3 μM TG. Maintenance of untreated cells in DMEM for the same time intervals resulted in progressive but moderate cell damage due to serum deprivation (open bars in Fig. 1).

Mitochondria have been found to play a primary role in the unfolding of certain apoptotic responses. Therefore, the subcellular distribution of cyt *c* was assessed when cells were undergoing apoptosis. Cyt *c* was detected by Western blotting in the S-10 and P-10 fractions. The S-10 fraction was the supernatant of a 10,000*g* centrifugation, once cells were selectively permeabilized with digitonin and the soluble content from the resulting pellet was the P-10 fraction. Before apoptosis was induced, i.e., at time zero, cyt *c* was present in the P-10 fraction but not in S-10 (Fig. 2). However, the induction of apoptosis gave rise to the time-dependent appearance of cyt *c* in the S-10 fraction. It was detectable as early as 1 h when 3 μM TG was used and after 30 min when 1 μg/ml TM was the death stimulus. Detection of COX IV protein indicated that the mitochondrial marker was only present in the P-10 fraction. This validates the cytosolic extract S-10 used in this study that was free of mitochondrial contamination. The blotting membrane was stripped and reprobed with anti-γ-tubulin to check that similar protein contents were in the lanes.

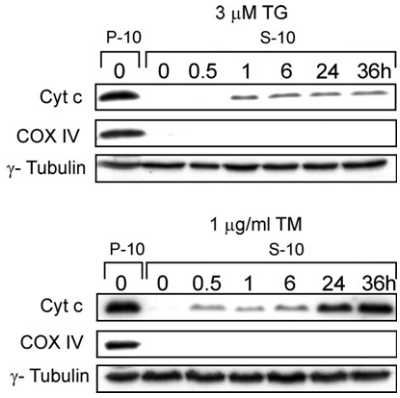

Fig. 2. Release of cyt *c* from mitochondria to cytosol was an early event in apoptosis induced by 3 μM TG or 1 μg/ml TM. Plated cells in DMEM were subjected to apoptotic treatment at 37 °C. After the indicated time periods, cells were treated with digitonin and the cellular fractions S-10 and P-10 were prepared. The 10,000*g* centrifugation permitted isolation of the cytosolic content in the supernatant since cells were selectively permeabilized with digitonin and not disrupted. Cyt *c* (p12), COX IV (p19.6) and γ-tubulin (p48) were detected by immunoblotting procedure in both fractions. γ-Tubulin was used as a protein loading control.

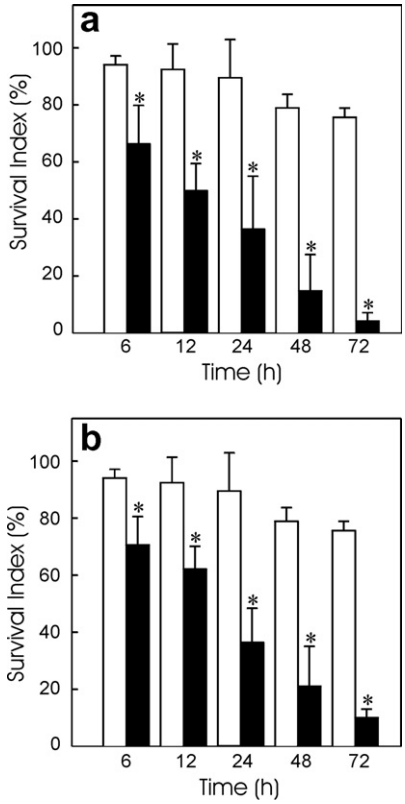

Fig. 1. Cellular damage induced by 3 μM TG (a) or 1 μg/ml TM (b) occurred in approximately the same time frame. Plated cells in DMEM were exposed at 37 °C to the apoptotic insult for different time periods (closed bars). Untreated cells in DMEM were also incubated for the same time intervals (open bars). Evaluation of the MTT reduction was carried out by colorimetric procedure. Data are expressed as a percentage with respect to a time zero control. Statistical significant effect of the apoptotic insult when treated cells were compared with untreated cells at the same incubation time (*).

The potential effect of a fast mitochondria depolarization as inducer of the observed redistribution of cyt *c* from mitochondria to cytosol was investigated with the aid of the cationic dye JC-1 and flow-cytometry experiments [18]. The accumulation of JC-1 in polarized mitochondria is known to be accompanied by a fluorescence shift of the probe from green to red [18]. So, a representative experiment indicated that the vast majority of untreated cells loaded with JC-1 emitted high red fluorescence consistent with an elevated inner mitochondrial membrane potential ($\Delta\Psi_m$) and only a small percentage exhibited lower values (Fig. 3a). Cells in regions R1 and R2 were 94% and 6%, respectively. The sensitivity of JC-1 to a $\Delta\Psi_m$ change was proved by treatment for 30 min with 5 μM carbonyl cyanide *m*-chlorophenylhydrazone (CCCP). Most of the cells showed a clear decrease of red emission fluorescence and a concomitant increase in green fluorescence when exposed to the uncoupling agent. In fact, cells in regions R1 and R2 after the treatment were 0.5% and 99.5%, respectively (Fig. 3b). Cells in region R1 were also evaluated at different time intervals after addition of 3 μM TG. Our data indicated that most of the cells were unaffected by the apoptotic treatment and remained in region R1 during the first 12 h although some decrease of the R1 population was

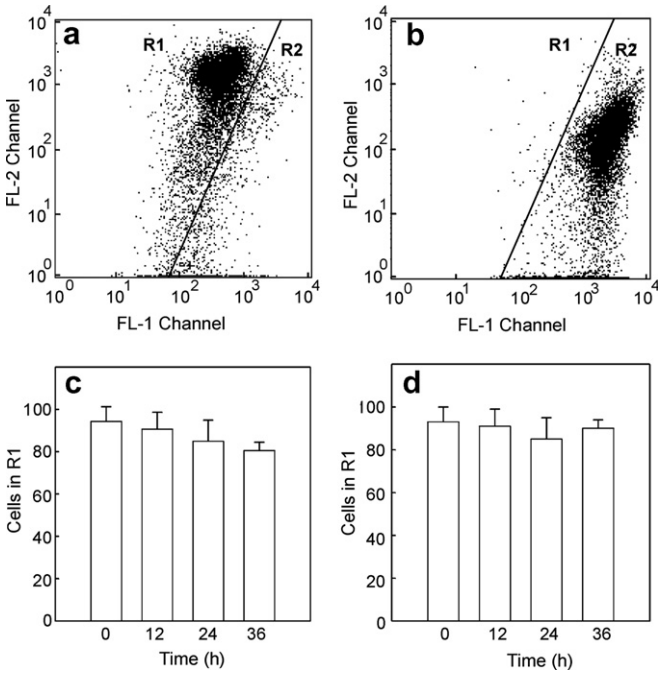

Fig. 3. Cells exposure to 3 μM TG or 1 μg/ml TM was not accompanied by collapse of $\Delta\Psi_m$. Plated cells in DMEM were exposed to the apoptotic insult. The incubation at 37 °C was extended for different time periods. Treated and untreated cells were loaded with the JC-1 probe and then trypsinized and resuspended. Measurements were carried out with a FACSort™ flow cytometer from BD. Green and red fluorescence was detected through the FL-1 and FL-2 channels, respectively. (a) Dots plot of untreated cells after appropriate electronic gating. Cells with high and low $\Delta\Psi_m$ are in region R1 and R2, respectively. (b) Dots plot of cells treated for 30 min with 5 μM CCCP to collapse the $\Delta\Psi_m$. (c) Time-dependent effect when cells were treated with 3 μM TG. (d) Time-dependent effect when cells were treated with 1 μg/ml TM.

developed at longer time intervals (Fig. 3c). When the apoptotic treatment was carried out in the presence of 1 μg/ml TM, the effect on cell population in R1 was negligible after 12 h and minimally affected after a period of 36 h (Fig. 3d).

The involvement of Bax as responsible for the mitochondrial release of cyt *c* has been documented in a number of experimental situations and cell types [24,25]. Therefore, the possibility of this mechanism for regulating cyt *c* release in our cell system was explored. The time course of Bax translocation to the mitochondria was monitored by Western blotting [26]. The cellular extract P-10 did not contain the Bax protein unless cells were previously treated with 3 μM TG or 1 μg/ml TM. Indeed, the appearance of Bax in the P-10 fraction was detectable after 30 min when either apoptotic inducers were used (Fig. 4).

This result prompted up to analyze Bax activation in H9c2 cells by confocal microscopy. To this end, cells were treated for different time intervals with 3 μM TG. Then, live treated and untreated cells were loaded with MitoTracker Red, a mitochondrial probe that can be detected as red fluorescence. The subsequent fixation and permeabilization processes allowed detection of active Bax with the aid of the primary antibody 6A7 [26]. Data presented correspond to

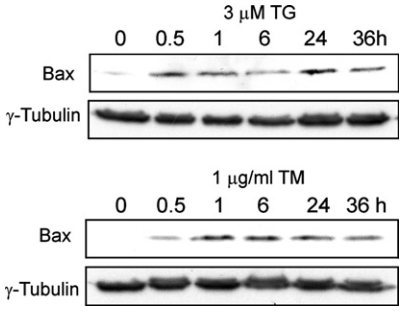

Fig. 4. Bax translocation to mitochondria was also an early event when cells were treated with 3 μM TG or 1 μg/ml TM. Plated cells in DMEM were treated at 37 °C with the appropriate apoptotic inducer. The time-dependent effect on Bax translocation was measured in the P-10 fraction after protein resolution and chemiluminescence detection of the immunoreactive band (p21). The γ-tubulin (p48) content was used as a control of the lanes loading.

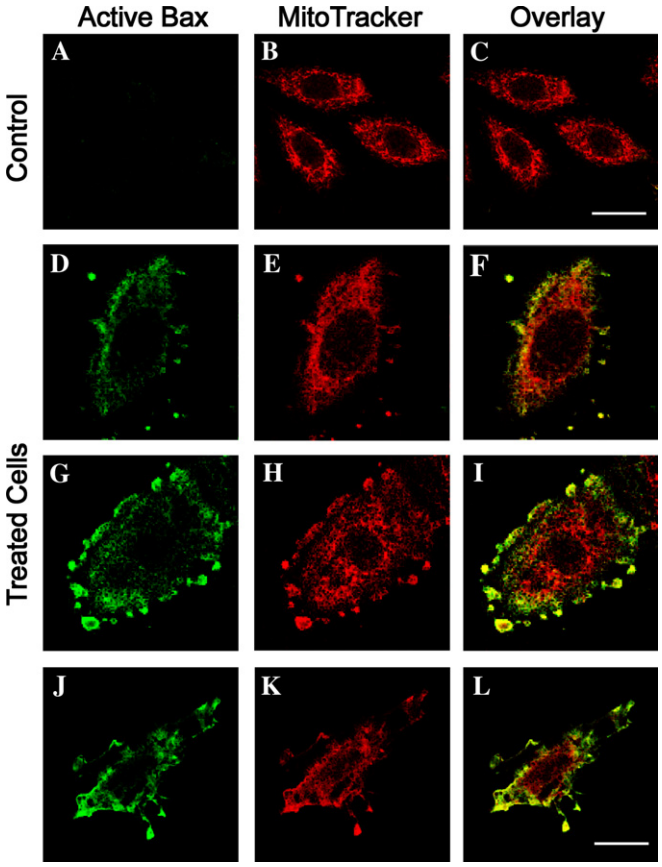

Fig. 5. Active Bax in dying cells had a preferential mitochondrial location and was more abundant at the cellular periphery. Images of laser confocal microscopy when plated cells were left untreated (A–C) or exposed to 3 μM TG (D–L). Cells were loaded with MitoTracker Red (red fluorescence) and treated for active Bax immunostaining (green fluorescence). The preferential location of active Bax in mitochondria was proved by the yellow color in the merged images of the right column (F, I and L). Images in each column were captured under the same sensitivity set up to allow comparison. Scale bar in C, also applicable to A and B, was 60 μm whereas in L, and also in D–K, was 20 μm.

individual cells engaged in apoptosis. As can be seen by the green fluorescence, active Bax was present in cells exposed to TG (Fig. 5D, G and J) but not in untreated cells

(Fig. 5A). Moreover, the distribution of Bax displayed a punctate pattern and was abundant at the cellular periphery but scarce in regions near the nucleus (Fig. 5D, G and J). The MitoTracker labeling of the cells provided a bright and dense network of red tiny spots distributed all over the confocal plane except on the nucleus (Fig. 5B, E, H and K). It is clear that Bax distribution overlapped in a large extent on the mitochondrial network as deduced when the corresponding images were superimposed (Fig. 5F, I and L).

The proteolytic activation of certain caspases is a distinctive characteristic of apoptosis induced by different death signals. Therefore, the participation of key caspases in response to the induced SR stress was analyzed. Caspase activation was monitored by Western blotting using antibodies that detected both procaspase and a cleaved fragment of the enzyme. Specifically, casp 12 was mainly detected as a p53 proform in the S-10 fraction of untreated cells although some basal level of the p35 fragment was also found (Fig. 6). The apoptotic treatment with either 3 μM TG or 1 μg/ml TM resulted in an increased accumulation of the cleaved fragment. Casp 12, that is predominantly associated to the SR membrane [27], was more clearly observed in the S-10 (Fig. 6) than in the P-10 fraction (data not shown) due to a lower number of unspecific bands in the blots. The S-10 fraction of untreated cells also contained the p32 proform of casp 3 but not the cleaved form (Fig. 6). Upon apoptosis induction, casp 3 was processed in a time-dependent manner to yield a detectable p17 fragment. Accumulation of the casp 3 proteolytic fragment occurred earlier when cells were treated with TG as compared with TM. Moreover, uncleaved casp 8 was present in the S-10 fraction as a p55 immunoreactive band and was processed after apoptosis induction to generate a p25 fragment (Fig. 6). In this case, accumulation of the cleaved fragment was only visible after a 24 h time span.

The significance of the mitochondrial release of cyt *c* and casp 3 activation in response to SR stress was examined in the presence of CsA or z-VAD-fmk. The optimal z-VAD-fmk inhibitory concentration was previously determined by measuring casp 3 activation. The assay was performed with the S-10 fraction and the exposure to 3 μM TG was for 6 h. Cells untreated or treated with TG were used to demonstrate the induced appearance of the p17 fragment. They served as negative and positive controls, respectively (Fig. 7a, first two lanes). When cells were preincubated for 1 h with increasing z-VAD-fmk concentrations before apoptotic induction the accumulation of the p17 fragment was progressively diminished. Full inhibition of casp 3 processing was obtained when the z-VAD-fmk concentration was above 10 μM.

As already shown, cyt *c* was absent in the S-10 fraction before but not after the treatment for 6 h with 3 μM TG (Fig. 7b, first two lanes; and also Fig. 2). Likewise, substantial processing of casp 3 was observed after the TG treatment but not before (Fig. 7b and also Fig. 6). Furthermore, cells preincubation for 10 min with 5 μM CsA did not block either the mitochondrial release of cyt *c* or the casp 3 activation. Nonetheless, preincubation for 1 h with 20 μM z-VAD-fmk failed to inhibit cyt *c* release but prevented casp 3 activation. An additional control assay indicated that preincubation with 5 μM CsA alone did not induce any response.

When parallel experiments were performed in the presence of 1 μg/ml TM for 24 h (Fig. 7c) the observed effects were similar to those described for 3 μM TG. Namely, cyt *c* appeared in the S-10 fraction of treated cells and processing of casp 3 was observed whereas neither release of cyt *c* nor casp 3 activation were observed in the S-10 fraction of untreated cells. Hence, 5 μM CsA added in preincubation did not alter either the mitochondrial release of cyt *c*

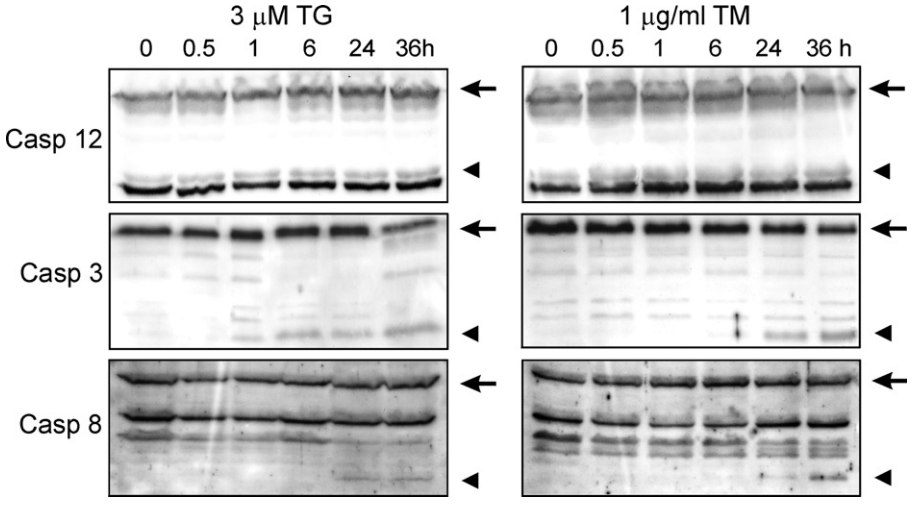

Fig. 6. Casp 12, casp 3 and casp 8 were activated when cells were exposed to 3 μM TG or 1 μg/ml TM. H9c2 cells were treated with the apoptotic stimulus for different time intervals. The time course of caspase activation was studied in the S-10 fraction. Uncleaved proforms of casp 12 (p53), casp 3 (p32) and casp 8 (p55) are marked with arrows. Detectable proteolytic fragments of casp 12 (p35), casp 3 (p17) and casp 8 (p25) are indicated by arrowheads. Unspecific bands in the blots are related with overexposure to detect the proteolytic cleavage of caspases.

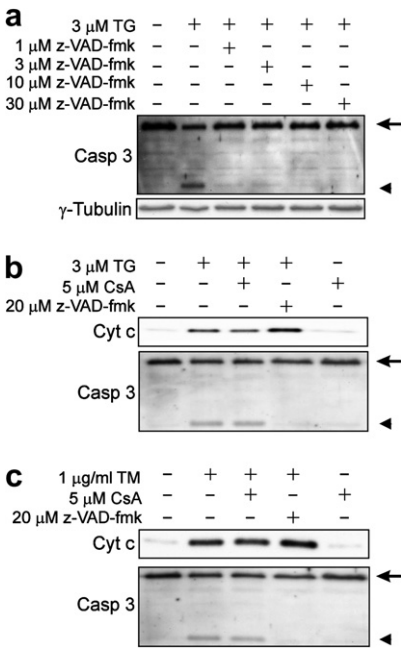

Fig. 7. CsA failed to prevent release of cyt *c* from mitochondria whereas z-VAD-fmk inhibited casp 3 activation. Cells were exposed for 6 h to 3 μM TG or 24 h to 1 μg/ml TM. In some experiments, cells were preincubated with 5 μM CsA for 10 min or a defined concentration of z-VAD-fmk for 1 h. Detection of cyt *c* (p12) and also uncleaved (p32) and cleaved casp 3 (p17) was sought in the S-10 fraction. (a) Casp 3 activation induced by 3 μM TG was studied in the presence of different z-VAD-fmk concentrations. γ-Tubulin (p48) was used as a loading control. (b) The effect of 3 μM TG on the mitochondrial release of cyt *c* and casp 3 activation was studied in the absence or after preincubation with 5 μM CsA or 20 μM z-VAD-fmk. (c) The effect of 1 μg/ml TM on cyt *c* release and casp 3 activation, in the absence or presence of CsA or z-VAD-fmk is shown.

or the casp 3 activation. In contrast, the 1 h preincubation with 20 μM z-VAD-fmk did not block cyt *c* release but prevented casp 3 activation. In the absence of apoptotic treatment, CsA had no effect when added in preincubation.

Selective inhibition of specific caspases may be a useful tool for identifying the relationship or hierarchy in the activation cascade. Here again, casp 3 activation induced by treatment for 6 h with 3 μM TG was considered. The positive but not the negative control revealed the p17 fragment that was detected in the S-10 fraction (Fig. 8 and also Fig. 6). However, the p17 fragment was not observed when cells were preincubated for 1 h with 20 μM z-LEHD-fmk, a selective inhibitor of casp 9, before exposure for 6 h to 3 μM TG. Interestingly, the same response was obtained when the preincubation was carried out in the presence of 20 μM z-IETD-fmk, a selective inhibitor of casp 8. It is also shown that following a 24 h exposure to 1 μg/ml TM, casp 3 activation was almost completely blocked when cells were preincubated for 1 h with either 20 μM z-LEHD-fmk or z-IETD-fmk.

In this regard, the effect of a selective casp 9 inhibitor on casp 8 activation was also analyzed. The apoptotic treatment for 36 h with 3 μM TG or 1 μg/ml TM as compared with the corresponding samples of untreated cells resulted in the accumulation of the p25 fragment (Fig. 8; see also Fig. 6). However, cells preincubation for 1 h with 20 μM z-LEHD-fmk before the 3 μM TG treatment precluded the appearance of the p25 fragment. Likewise, 1 h preincubation with 20 μM z-LEHD-fmk substantially blocked the proteolytic cleavage of casp 8 when the apoptotic inducer was 1 μg/ml TM.

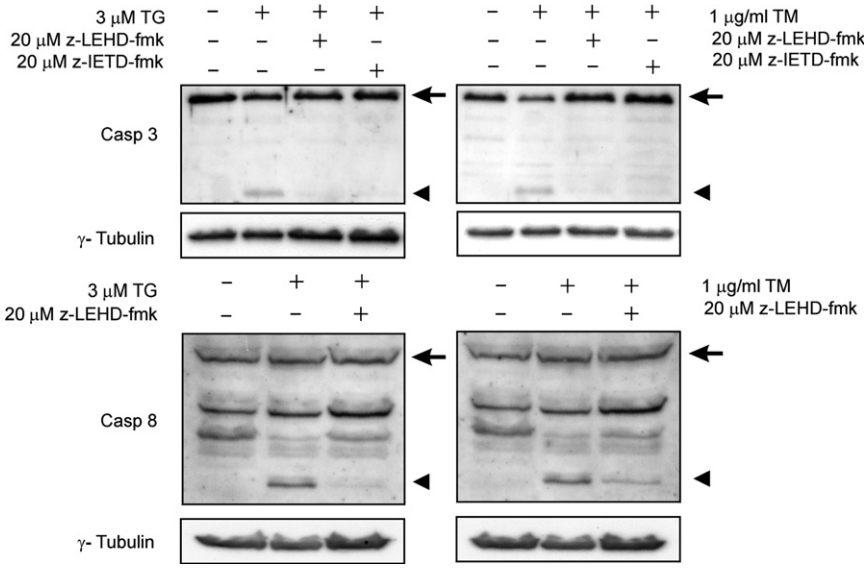

Fig. 8. Either z-LEHD-fmk or z-IETD-fmk prevented activation of casp 3 whereas z-LEHD-fmk also blocked casp 8 activation. For the study of casp 3, plated cells were treated for 6 h with 3 μM TG or 24 h with 1 μg/ml TM (upper panels). Casp 8 activation was studied after 36 h treatment with either apoptotic inducers (lower panels). In some experiments, the apoptotic treatment was preceded by preincubation with a specific (cell-permeable and irreversible) caspase inhibitor for 1 h. Both, casp 3 and casp 8 were studied in the S-10 fraction. Proforms of casp 3 (p32) and casp 8 (p55) are marked with arrows. Detectable fragments of cleaved casp 3 (p17) and casp 8 (p25) are marked with arrowheads. The γ-tubulin (p48) content in each lane was a loading control.

Apoptosis induced by irreversible SR stress is intimately connected to proteolytic cleavage of relevant caspases therefore it was important to evaluate whether blockade of caspase activation protected against cell death. H9c2 cells subjected to apoptotic treatment for different time intervals were taken as a reference and compared with cells pretreated for 1 h with 20 μM z-VAD-fmk before the apoptosis insult. The cellular damage was evaluated by measuring the MTT reductase activity. The viability of cells treated with 3 μM TG was progressively diminished as a function of time (closed bars in Fig. 9a; see also Fig. 1a). Notably, preincubation with 20 μM z-VAD-fmk did not result in cell protection and the time-dependent profile was similar to that obtained in the absence of general caspase inhibitor (cf. gray bars and closed bars in Fig. 9a). As a reference, values of untreated cells at each time point were also included (open bars). Similar to data obtained in the presence of TG, the time-dependent decline in the redox potential when cells were exposed to 1 μg/ml TM was not protected by preincubation with the cell-permeable and irreversible general caspase inhibitor (Fig. 9b).

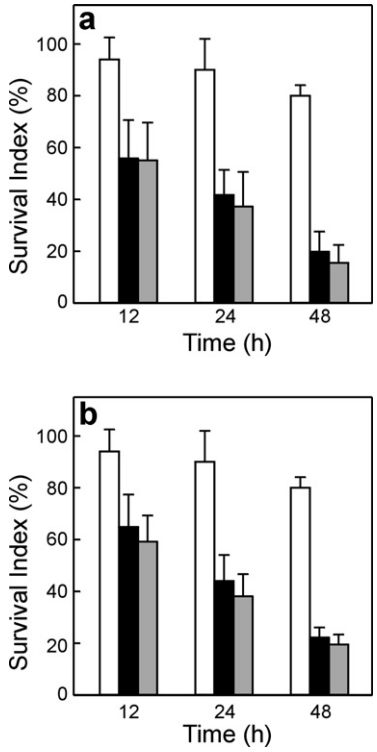

Fig. 9. Caspase inhibition in H9c2 cells did not confer cytoprotection. Plated cells in DMEM were exposed at 37 °C to 3 μM TG (a) or 1 μg/ml TM (b). Cell viability was evaluated by the MTT assay. Cells were treated for different time periods (closed bars), or were preincubated for 1 h with 20 μM z-VAD-fmk before treatment (gray bars). Untreated cells in DMEM were also maintained for the same time intervals (open bars). Differences at each incubation time between cells subjected to apoptotic treatment in the presence or absence of z-VAD-fmk did not reach statistical significance ($p > 0.05$).

Discussion

The experimental discharge of the SR Ca^{2+} pool by TG or the interference with the *N*-glycosylation of proteins in the SR by TM provoked similar time-dependent cell damage in H9c2 cells (Fig. 1). The question then arises as to whether two different death signals acting on the same organelle share the same apoptotic response.

When cells were exposed to 3 μM TG or 1 μg/ml TM the release of mitochondrial cyt *c* was an early event (Fig. 2) while the observed decrease of $\Delta\Psi_m$ in the whole cell population was small and occurred later (Fig. 3). This indicated that cyt *c* release associated with SR stress was not induced by depolarization of the inner mitochondrial membrane. Indeed, pretreatment with CsA to block the permeability transition pore (PTP) had no effect to prevent cyt *c* release (Fig. 7b and c).

Bax and Bak activation in both mitochondria and ER are essential components of the ER-mediated apoptotic process [28,29]. In this regard, data presented herein indicated that Bax activation and translocation to the outer mitochondrial membrane occurred in the early stages of apoptosis when H9c2 cells were subjected to SR damage (Figs. 4 and 5).

Intense or prolonged ER stress as that induced by TG or TM is initially sensed by the ER membrane proteins PERK, IRE1 and ATF6 that eventually activate downstream signaling pathways and the commitment to death is mediated by intermediary molecules such as CHOP, JNK and proteins of the Bcl-2 family [30]. An essential unresolved issue is how the multiple components of the apoptotic machinery are integrated and timed in response to the ER stress. So far, it is unclear whether there is one defined proapoptotic event that controls all others or there are different events that simultaneously function to activate the cell death process. In any case, the current experimental models rely on chemical agents that induce synchronous and severe ER damage. Therefore, under conditions of high stress levels as those imposed by TG or TM, the apoptotic responses triggered by both agents share the same basic events. This is not to say that moderated ER stress signals experienced by cells "in vivo" cannot proceed through different pathways and cannot give rise to different apoptotic responses.

The activation of casp 12 in mouse fibroblasts under the presence of TG or TM and the partial suppression of apoptosis in casp 12-deficient cells [27] favored the idea that casp 12 could be the initiator caspase in rodents. Other studies indicated that z-VAD-fmk inhibited processing of casp 12 but not casp 9 and casp 3 under the presence of TG [31] pointing to a relevant role of mitochondria. More recent studies confirmed that ER stress-induced apoptosis can be developed in the absence of casp 12 [32,33]. The involvement of other mediators such as calpains, death receptors, the caspase-independent pathway, etc. has also been described. Our data indicate that casp 12 processing was stimulated shortly after induction of the SR damage (Fig. 6) and the release of mito-

chondrial cyt *c* could be observed in the presence of z-VAD-fmk (Fig. 7b and c). Therefore, activation of cell death was caspase-independent and the decisive event that marks the ''point of no return'' in the lethal process occurred upstream. Moreover, Bax translocation to the mitochondria occurred before or at the time of cyt *c* release (cf. Figs. 2 and 4). Consistent with these results, the early participation of mitochondria without a loss of $\Delta\Psi_m$ in apoptosis induced by SR damage can be established.

Once the initiator caspases are activated they act on downstream effector caspases which are responsible in a large extent for the rapid and ordered dismantling of the cell. Activation of casp 9 subsequent to cyt *c* release was undetectable in our experimental system using commercially available antibodies (data not shown), however, activation of casp 3 and casp 8 was patent (Fig. 6). In this connection, casp 3 activation and cyt *c* release were independent of PTP opening and the general caspase inhibitor abolished casp 3 activation but not mitochondrial release of cyt *c* (Fig. 7b and c), confirming that casp 3 was activated downstream of cyt *c* release. Furthermore, the inhibitory dependence generated under the presence of a selective casp 9 or casp 8 inhibitor indicates that casp 3 activation was abrogated by inhibition not only of casp 9, as can be expected, but also of casp 8 (Fig. 8). This suggests that casp 3 was in the same sequence of events and in some way downstream of casp 9 and casp 8. The sensitivity of casp 8 activation to a selective casp 9 inhibitor (Fig. 8) lends support to the idea that casp 8 was downstream of casp 9 and casp 3. These findings indicate that casp 3 and casp 8 are engaged in a mitochondrial amplification loop aimed at potentiating the execution phase of apoptosis as already described in other experimental systems [34,35].

Inhibition of caspase cleavage in cardiomyocytes has been associated with resistance to cell death as assessed by the study of parameters related with DNA fragmentation [36,37]. However, z-VAD-fmk did not protect against cell damage when the viability parameter was measured (Fig. 9) confirming that cell death is not necessarily linked to caspase activation. It should be noted that the release of mitochondrial cyt *c* from the intermembrane space is accompanied by the release of AIF and other caspase-independent death effectors [38]. This alternative mechanism that exhibits distinctive morphological features is considered responsible for a switch from canonical apoptosis to other forms of cell death including necrosis [38].

Caspases are main players of apoptosis but do not exert the control when induced by SR damage. A key question to uncover is the identity of the molecular event triggering the onset of apoptosis.

Acknowledgments

This study was funded by Grant BCM2002-02474 from the Spanish Ministerio de Educación y Ciencia/ Fondo Europeo de Desarrollo Regional and by a grant-in-aid from the Universidad de Murcia.

References

[1] N.N. Danial, S.J. Korsmeyer, Cell 116 (2004) 205–219.
[2] A. Ashkenazi, V.M. Dixit, Science 281 (1998) 1305–1308.
[3] X. Wang, Genes Dev. 15 (2001) 2922–2933.
[4] K.F. Ferri, G. Kroemer, Nat. Cell Biol. 3 (2001) E255–E263.
[5] S.R. Datta, A. Brunet, M.E. Greenberg, Genes Dev. 13 (1999) 2905–2927.
[6] W. Cheng, J. Kajstura, J.A. Nitahara, B. Li, K. Reiss, Y. Liu, W.A. Clark, S. Krajewski, J.C. Reed, G. Olivetti, P. Anversa, Exp. Cell Res. 226 (1996) 316–327.
[7] R.A. Gottlieb, K.O. Burleson, R.A. Kloner, B.M. Babior, R.L. Engler, J. Clin. Invest. 94 (1994) 1621–1628.
[8] E. Teiger, T.V. Dam, L. Richard, C. Wisnewsky, B.S. Tea, L. Gaboury, J. Tremblay, K. Schwartz, P. Hamet, J. Clin. Invest. 97 (1996) 2891–2897.
[9] V.G. Sharov, H.N. Sabbah, H. Shimoyama, A.V. Goussev, M. Lesch, S. Goldstein, Am. J. Pathol. 148 (1996) 141–149.
[10] S.E. Logue, A.B. Gustafsson, A. Samali, R.A. Gottlieb, J. Mol. Cell Cardiol. 38 (2005) 21–33.
[11] D.T. Rutkowski, R.J. Kaufman, Trends Cell Biol. 14 (2004) 20–28.
[12] Y. Sagara, G. Inesi, J. Biol. Chem. 266 (1991) 13503–13506.
[13] N.A. Turner, F. Xia, G. Azhar, X. Zhang, L. Liu, J.Y. Wei, J. Mol. Cell Cardiol. 30 (1998) 1789–1801.
[14] Y. Mizukami, S. Kobayashi, F. Uberall, K. Hellbert, N. Kobayashi, K. Yoshida, J. Biol. Chem. 275 (2000) 19921–19927.
[15] C.-Y. Huang, W.-W. Kuo, P.J. Chueh, C.-T. Tseng, M.-Y. Chou, J.-J. Yang, Biochem. Biophys. Res. Commun. 324 (2004) 424–431.
[16] B.W. Kimes, B.L. Brandt, Exp. Cell Res. 98 (1976) 367–381.
[17] A. Lax, F. Soler, F. Fernandez-Belda, J. Bioenerg. Biomembr. 37 (2005) 249–259.
[18] A. Cossarizza, M. Baccarani-Contri, G. Kalashnikova, C. Franceschi, Biochem. Biophys. Res. Commun. 197 (1993) 40–45.
[19] R.A. Gottlieb, D.J. Granville, Methods 26 (2002) 341–347.
[20] P.K. Smith, R.I. Krohn, G.T. Hermanson, A.K. Mallia, F.H. Gartner, M.D. Provenzano, E.K. Fujimoto, N.M. Goeke, B.J. Olson, D.C. Klenk, Anal. Biochem. 150 (1985) 76–85.
[21] U.K. Laemmli, Nature 227 (1970) 680–685.
[22] M. Rossner, K.M. Yamada, J. Cell Biol. 166 (2004) 11–15.
[23] A. Lax, F. Soler, F. Fernandez-Belda, Biochim. Biophys. Acta 1763 (2006) 937–947.
[24] S. Manon, B. Chaudhuri, M. Guérin, FEBS Lett. 415 (1997) 29–32.
[25] R. Eskes, B. Antonsson, A. Osen-Sand, S. Montessuit, C. Richter, R. Sadoul, G. Mazzei, A. Nichols, J.C. Martinou, J. Cell Biol. 143 (1998) 217–224.
[26] O. Tikhomirov, G. Carpenter, J. Cell Sci. 118 (2005) 5681–5690.
[27] T. Nakagawa, H. Zhu, N. Morishima, E. Li, J. Xu, B.A. Yankner, J. Yuan, Nature 403 (2000) 98–103.
[28] M.C. Wei, W.-X. Zong, E.H.-Y. Cheng, T. Lindsten, V. Panoutsakopoulou, A.J. Ross, K.A. Roth, G.R. MacGregor, C.B. Thompson, S.J. Korsmeyer, Science 292 (2001) 727–730.
[29] L. Scorrano, S.A. Oakes, J.T. Opferman, E.H. Cheng, M.D. Sorcinelli, T. Pozzan, S.J. Korsmeyer, Science 300 (2003) 135–139.
[30] E. Szegezdi, S.E. Logue, A.M. Gorman, A. Samali, EMBO Rep. 7 (2006) 880–885.
[31] Y. Kitamura, A. Miyamura, K. Takata, M. Inden, D. Tsuchiya, K. Nakamura, T. Taniguchi, J. Pharmacol. Sci. 92 (2003) 228–236.
[32] E.A. Obeng, L.H. Boise, J. Biol. Chem. 280 (2005) 29578–29587.
[33] F. Di Sano, E. Ferraro, R. Tufi, T. Achsel, M. Piacentini, F. Cecconi, J. Biol. Chem. 281 (2006) 2693–2700.
[34] E.A. Slee, S.A. Keogh, S.J. Martin, Cell Death Differ. 7 (2000) 556–565.
[35] D. Tang, J.M. Lahti, V.J. Kidd, J. Biol. Chem. 275 (2000) 9303–9307.
[36] T.L. Yue, C. Wang, A.N. Romanic, K. Kikly, P. Keller, W.E. DeWolf Jr, T.K. Hart, H.C. Thomas, B. Storer, J.L. Gu, X. Wang, G.Z. Feuerstein, J. Mol. Cell Cardiol. 30 (1998) 495–507.
[37] T.A. Holly, A. Drincic, Y. Byun, S. Nakamura, K. Harris, F.J. Klocke, V.L. Cryns, J. Mol. Cell Cardiol. 31 (1999) 1709–1715.
[38] G. Kroemer, S.J. Martin, Nat. Med. 11 (2005) 725–730.